JACS
JOURNAL OF THE AMERICAN CHEMICAL SOCIETY

Communication

pubs.acs.org/JACS

Shape Control from Thermodynamic Growth Conditions: The Case of hcp Ruthenium Hourglass Nanocrystals

John Watt,[†] Chenlong Yu,[†] Shery L. Y. Chang,[‡] Soshan Cheong,[†,§] and Richard D. Tilley[†,*]

[†]School of Chemical and Physical Sciences and The MacDiarmid Institute for Advanced Materials and Nanotechnology, Victoria University of Wellington, Wellington 6012, New Zealand

[‡]Monash Centre for Electron Microscopy, Monash University, Clayton, Australia

[§]Industrial Research Limited, P.O. Box 31-310, Lower Hutt 5040, New Zealand

Supporting Information

ABSTRACT: Recent successes in forming different shaped face centered cubic (fcc) metal nanostructures has enabled a greater understanding of nanocrystal growth mechanisms. Here we extend this understanding to the synthesis of hexagonally close packed (hcp) metal nanostructures, to form uniquely faceted ruthenium nanocrystals with a well-defined hourglass shape. The hourglass nanocrystals are formed in a three-step thermodynamic growth process with dodecylamine as the organic stabilizer. The hourglass nanocrystals are then shown to readily self-assemble to form a new type of nanocrystal superlattice.

Great advances have been made in designing synthetic methods for the formation of a range of unique shapes in metal nanocrystal synthesis, for example branched, overgrown, and porous nanostructures from face centered cubic (fcc) metals such as Pd, Pt, and Au.[1−3] However methods are less well established for metals with the hexagonal closed packed (hcp) crystal structure. Due to the huge potential of ruthenium as a catalyst in aromatic hydrogenation and CO oxidation, the formation of different shaped ruthenium nanocrystals is also an area of great interest.[4,5] Recent work by Zhou et al. and Hoefelmeyer et al. has produced branched ruthenium nanocrystals, and Banin et al. have synthesized ruthenium nanocages; however the majority of syntheses have led to spherical or near-spherical nanocrystals, as well as their aggregates.[6−11] Because ruthenium crystallizes in an hcp crystal structure, methods used to control the shape of fcc noble metal nanocrystals cannot be readily applied. This is largely due to an inherent anisotropy in the hcp crystal structure which promotes growth in the direction of the *c*-axis, leading to rod or worm-like nanostructures.[10] Synthetic shape control in the formation of ruthenium nanocrystals therefore remains an important challenge, combined with a need for an understanding of the growth mechanisms.

In order to effectively investigate and exploit the promising properties of different shaped metal nanocrystals, a uniform shape and narrow size distribution is essential.[12] Such uniformity can be achieved in a relatively facile manner when nanocrystals are formed in the solution phase under slow, thermodynamically controlled growth conditions.[13] However, shape control of metal nanocrystals grown in the solution phase can often be fast and kinetically controlled.[14,15] Therefore, the development of thermodynamically driven synthetic methods to achieve shape control for hcp metals could allow for a range of well-defined, uniquely shaped nanocrystals.

Here we report the formation of uniquely shaped ruthenium hourglass nanocrystals from a thermodynamically controlled growth regime. To synthesize the hourglass nanocrystals, ruthenium(II) acetylacetonate is reacted in a pressure reaction vessel under a hydrogen atmosphere for 70 h with dodecylamine as the organic stabilizer ligand. During their formation we observe a three-step growth process: (i) coalescence of ruthenium nanoparticle nuclei to form partially crystalline rod-like nanoparticles, (ii) crystallization, and (iii) overgrowth to form well-defined and uniform hourglass nanocrystals. The hourglass nanocrystals are observed to readily self-assemble with spherical ruthenium nanocrystals to form a shape-directed nanocrystal superlattice.

Figure 1a shows a typical transmission electron microscope (TEM) image of the ruthenium hourglass nanocrystals. The hourglass nanocrystals are 18 ± 3 nm in length and 11 ± 2 nm wide with necks that are 4 ± 1 nm thick (full size distribution analysis is given in the Supporting Information (SI), Figure S1). They were synthesized in a yield of 77% with the remainder made up of 19% rod-like and 4% near-spherical nanocrystals.

Figure 1b shows a high resolution transmission electron microscope (HRTEM) image of a single ruthenium hourglass nanocrystal. The hourglass is 18 nm in length and 13 nm wide with a 4 nm wide neck. The fast Fourier transform (FFT) of the image is shown in Figure 1c with spots assigned as {002}, {101}, and {100} reflections, indicating the hourglass is single crystal hcp viewed down a ⟨010⟩ orientation. The hourglass nanocrystal is bound by {001} and {101} facets at the ends and sides respectively, and the truncated corners of the hourglass are terminated by {101} facets. This is shown schematically in Figure 1d. The shape of the hourglass is analogous to two truncated hexagonal pyramid subunits joined at their vertices (for further analysis, see SI S2).

The hourglass shape is different from ruthenium and cobalt hexagonal platelets where selective adsorption of capping ligands or counterions on the (001) hcp facet has been observed to form hexagonal platelets and stacked platelet

Received: November 19, 2012
Published: December 26, 2012

dx.doi.org/10.1021/ja311366k | *J. Am. Chem. Soc.* 2013, 135, 606−609

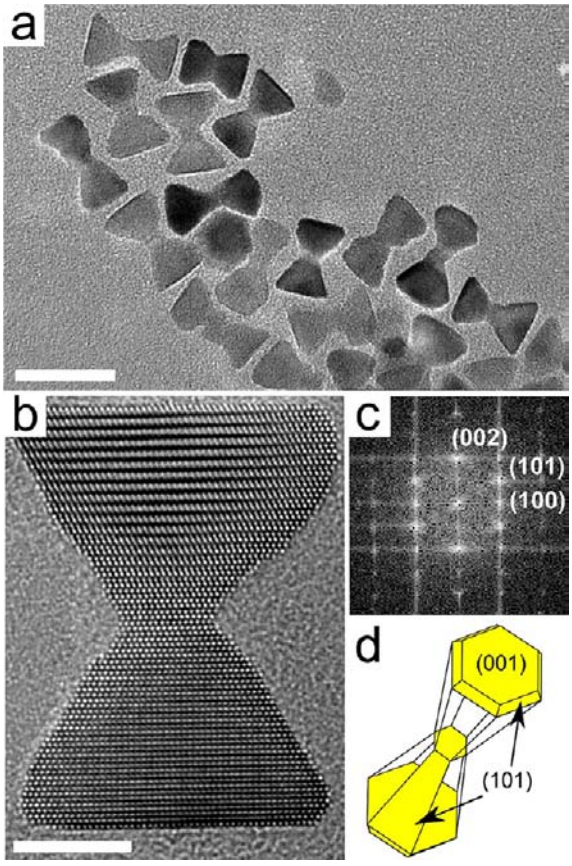

Figure 1. Ruthenium hourglass nanocrystals synthesized after 70 h. (a) TEM image of ruthenium hourglass nanocrystals, scale bar = 20 nm. (b) HRTEM image of a single, highly crystalline, ruthenium hourglass nanocrystal, scale bar = 5 nm. (c) FFT of the ruthenium hourglass nanocrystal shown in (b). (d) Schematic of a single ruthenium hourglass nanocrystal showing termination by {001} and {101} facets.

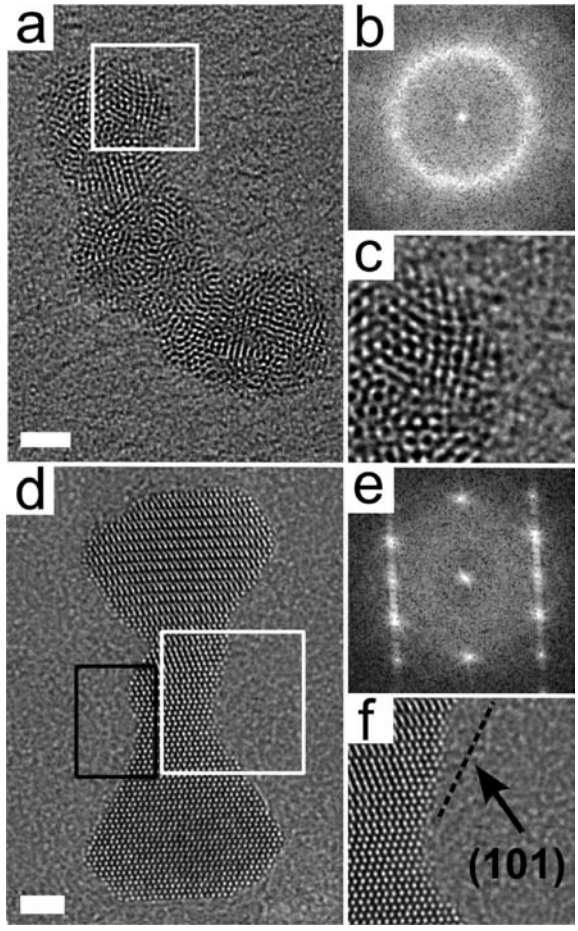

Figure 2. Ruthenium hourglass nanocrystal intermediates. (a) HRTEM image of a partially crystalline ruthenium rod-like nanocrystal intermediate isolated after 48 h, scale bar = 2 nm. (b) FFT of the ruthenium rod-like nanocrystal shown in (a). (c) High magnification HRTEM image of the surface of the rod-like nanocrystal as shown by the white box in (a). (d) HRTEM image of a single crystal ruthenium hourglass-like nanocrystal intermediate isolated after 52 h, scale bar = 2 nm. (e) FFT of the ruthenium hourglass-like nanocrystal shown in (d). (f) High magnification HRTEM image of the surface of the hourglass-like nanocrystal as shown by the white box in (d). The selected area of the surface indicated by the black box is further analyzed in Figure 3.

shapes.[16] The ruthenium hourglass nanocrystals retained their shape after aging for 140 h at 140 °C, illustrating the stability of this morphology (SI, Figure S3).

To investigate the role of the stabilizer, ligand experiments were performed with oleylamine or hexadecylamine replacing the dodecylamine (SI, Figure S4). When oleylamine or hexadecylamine was used only irregular shaped nanocrystals were formed, indicating dodecylamine is critical for the growth of ruthenium hourglass nanocrystals. To understand the growth of the hourglass nanocrystals, intermediates were isolated by quenching the reaction at 20, 48, and 52 h. After 20 h near-spherical partially crystalline ruthenium nanocrystal nuclei (3.9 ± 0.6 in size) were isolated (see SI, Figure S5). The inset in Figure S5 shows a selected area electron diffraction (SAED) pattern that has diffuse rings indicating the nanocrystal nuclei are only partially crystalline.

Figure 2a shows an HRTEM image of an intermediate nanocrystal isolated after 48 h. The intermediate is 15 nm in length and 5 nm wide and consists of 3 nanoparticle nuclei coalesced in a bent-chain formation. The FFT of the image is given in Figure 2b which shows a slightly diffuse ring corresponding to {101} reflections, indicating a partially crystalline structure. A close-up of the intermediate nanocrystal surface is shown in Figure 2c. The surface is rounded with no assignable terminating facets observable. Figure 2d shows an intermediate nanocrystal isolated after 52 h. The intermediate is 18 nm in length and 9 nm wide with an overall shape resembling an hourglass. The FFT of the image is given in Figure 2e with spots assigned as {002}, {101}, and {100} reflections, which indicates the intermediate is single crystal hcp viewed down a ⟨010⟩ zone axis. The intermediate nanocrystal surface is comprised of {001} and {101} facets with regions of higher index facets observable. This is confirmed by a high magnification HRTEM image of the surface (Figure 2f). The dotted line in Figure 2f shows that {101} facets are yet to form, indicating the intermediate is still experiencing growth. The observation of a residual ruthenium precursor after purification of the intermediates confirms that growth continues from the intermediate to form the final hourglass nanocrystals. In order to better understand the structure of the intermediate a selected area of the surface (shown by the black box in Figure 2d) was examined with aberration corrected HRTEM, shown in Figure 3.

The high magnification HRTEM image shows an area of the intermediate surface which is terminated by {110} facets with a

dx.doi.org/10.1021/ja311366k | J. Am. Chem. Soc. 2013, 135, 606−609

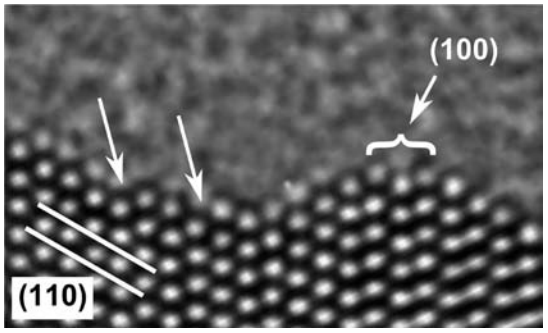

Figure 3. High magnification HRTEM image of the surface of an hourglass-like intermediate. The arrows point to $n(110) \times (110)$ type monatomic steps and the curly bracket shows a (110)/(110) type edge reconstructed to form a (100) surface.

number of surface defects observable. All the additional nanocrystals analyzed by HRTEM (for example, SI, Figure S6) indicate the formation of (110) facets. Employing a notation developed for the surface analysis of Pt nanocrystals, the arrows point to monatomic $n(110) \times (110)$ type steps.[17,18] The (110)/(110) edge labeled by the curly bracket has reconstructed to give a (100) type surface. These defects create a surface with a higher energy when compared to a clean {110} terminated surface indicating further growth occurs to form the final well-defined hourglass nanocrystals.

From HRTEM analysis of the time-resolved experiments we observe three distinct growth steps: (i) coalescence, (ii) crystallization, and (iii) overgrowth. The first step involves the coalescence of spherical ruthenium nuclei to form partially crystalline rod-like nanoparticles. The observation of coalescence is well established in nanoparticles synthesis, for example in the formation of Au and Pt nanocrystals, and is driven by a reduction in the surface free energy.[19,20]

In the second stage, the partially crystalline rod-like nanoparticles crystallize into single crystal structures as shown in Figure 2d. Such crystallization following coalescence has previously been observed in the formation of Pt nanocrystals and ZnO nanorods.[21−23] The thermodynamic driving force for crystallization in the current system is thought to be an increase in metal−metal bonding which offsets the entropic cost of eliminating crystal defects. This is due to the relatively high metal−metal bonding strength of ruthenium when compared to other metals, e.g., Pt or Pd.[24,25]

The third and final growth step involves further growth to form well-defined hourglass nanocrystals. For hcp structures the expression of (001) and (101) facets is energetically preferred as these have the highest atomic density and are therefore considered the lowest energy facets ($\rho(001) > \rho(101) > \rho(100)$).[26,27] Therefore as the single crystal intermediates continue to grow and atoms rearrange, surface coverage by low energy (001) and (101) facets is increased at the expense of relatively high energy (100) type facets leading to a well-defined hourglass shape. The stabilization energy of the (101) is enough to offset any energy cost due to the neck. A critical size of neck may be necessary, as no hourglass nanocrystals were observed with necks below 3 nm. Also observed (~4% yield) were ruthenium bowtie-like nanocrystals with two necks (SI, Figure S7). It is thought this is due to larger nanocrystal nuclei positioned in the middle of the orientated attachment process in step one. The growth of the hourglass nanocrystals is further encouraged by the presence of dodecylamine as the capping ligand. Dodecylamine is a straight chain organic molecule with 12 carbon atoms which can close-pack on a surface.[28] Due to an increased packing density, (001) and (101) type facets can accommodate a more dense coverage of dodecylamine. This leads to reduction in the surface energy of the nanocrystal due to an increase in the number of interactions between the dangling bonds of surface ruthenium atoms and the amine functionality of the surfactant. In contrast oleylamine has a kink in its carbon chain due to the double bond decreasing the ability of the stabilizer to close-pack on the surface, leading to less surface stabilization and irregular shaped nanocrystals. Hexadecylamine also forms irregular nanocrystals; this is because longer chain organic stabilizers are known to bind less strongly than those with a chain length of 12 carbon atoms to nanocrystal surfaces.[29] A similar process was observed in the thermodynamically controlled growth of fcc Pt_3Fe nanorods where redistribution following coalescence decreased the overall surface energy to form smooth, well-defined and straight nanorods.[30] In the current system we observe the same reduction in surface energy, as low energy facets are preferentially exposed. For fcc structures this typically leads to shapes bound by {111} and {100} facets; however for the hcp crystal structure, {001} and {101} facets are energetically preferred leading to an hourglass shape.[14,31]

The ruthenium hourglass nanocrystals are uniform in shape and size and were therefore considered as good candidates for self-assembly. A solution containing a mixture of spherical and hourglass shaped ruthenium nanocrystals was dried on a TEM grid. The nanocrystals readily self-assembled to form a new type of nanocrystal superlattice, shown in Figure 4 with a schematic in the inset. The unit cell shows a 2:1 ratio of hourglass to spherical nanocrystals. The maximum superlattice observed was 0.05 μm^2. Additional regions of self-assembly with the same structure are shown in Figure S8 with no other superlattice structures observed. The binary superlattice consists of ruthenium hourglass nanocrystals in horizontal and vertical orientations with spherical ruthenium nanocrystals incorporated in the interstices. The interparticle spacing for the vertically oriented hourglass is 1.9 nm and is consistent with overlapping dodecylamine.

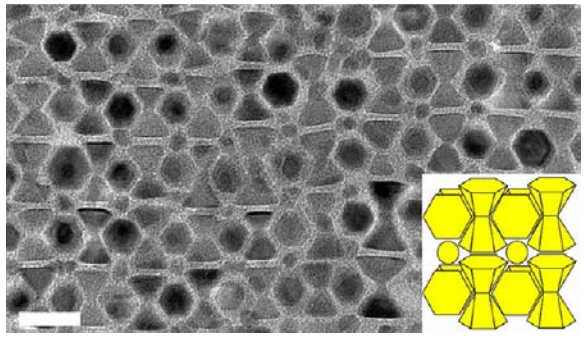

Figure 4. TEM image of a binary nanocrystal superlattice formed by the controlled evaporation of a mixture of ruthenium hourglass nanocrystals and spherical ruthenium nanocrystals. Scale bar = 20 nm.

In summary, we have formed ruthenium nanocrystals with a well-defined hourglass shape from thermodynamic growth conditions. Intermediates were isolated which show that the nanocrystals grow in a three-step process involving (i) coalescence, (ii) crystallization, and (iii) overgrowth. Each step is driven by a reduction in the overall nanocrystal free

dx.doi.org/10.1021/ja311366k | J. Am. Chem. Soc. 2013, 135, 606−609

energy. The ruthenium hourglass nanocrystals are then shown to readily self-assemble to form a new type of shape-directed nanocrystal superlattice. These results show that concepts of thermodynamic growth developed to form highly faceted fcc nanocrystals can be applied to hcp metals to produce an entirely new shape of nanocrystal. This opens up the possibility of forming a whole range of uniquely shaped nanocrystals for hcp metals where different crystal faces are thermodynamically stabilized and exposed on the surface. Such new types of nanocrystals will undoubtedly display unique catalytic, optical, and electronic properties.

■ ASSOCIATED CONTENT

Supporting Information

Full experimental details, size distribution analysis, and additional TEM can be found in the Supporting Information. This material is available free of charge via the Internet at http://pubs.acs.org.

■ AUTHOR INFORMATION

Corresponding Author

richard.tilley@vuw.ac.nz

Notes

The authors declare no competing financial interest.

■ ACKNOWLEDGMENTS

R.D.T., J.W., and S.C. thank the MacDiarmid Institute and MBIE for funding through Grant CONT-29690-HVMSSI-VICLINK and CONT-20707-NMTS-IRL.

■ REFERENCES

(1) Watt, J.; Young, N.; Haigh, S.; Kirkland, A.; Tilley, R. D. *Adv. Mater.* **2009**, *21*, 2288−2293.

(2) Cheong, S.; Watt, J.; Ingham, B.; Toney, M. F.; Tilley, R. D. *J. Am. Chem. Soc.* **2009**, *131*, 14590−14595.

(3) Vigderman, L.; Zubarev, E. R. *Langmuir* **2012**, *28*, 9034−9040.

(4) Joo, S. H.; Park, J. Y.; Russell Renzas, J.; Butcher, D. R.; Huang, W.; Somorjai, G. A. *Nano Lett.* **2010**, *10*, 2709−2713.

(5) Garcia-Anton, J.; Rosa Axet, M.; Jansat, S.; Philippot, K.; Chaudret, B.; Pery, T.; Buntowsky, G.; Limbach, H.-H. *Angew. Chem., Int. Ed.* **2008**, *47*, 2074−2078.

(6) (a) Lignier, P.; Bellabarba, R.; Tooze, R. P.; Su, Z.; Landon, P.; Menard, H.; Zhou, W. *Cryst. Growth Des.* **2012**, *12*, 939−942. (b) Chakroune, N.; Viau, G.; Ammar, S.; Poul, L.; Veautier, D.; Chehimi, M. M.; Mangeney, C.; Villain, F.; Fievet, F. *Langmuir* **2005**, *21*, 6788−6796.

(7) Vanden Brink, M.; Peck, M. A.; More, K. L.; Hoefelmeyer, J. D. *J. Phys. Chem. C* **2008**, *112*, 12122−12126.

(8) Macdonald, J. E.; Bar Sadan, M.; Houben, L.; Popov, I.; Banin, U. *Nat. Mater.* **2010**, *9*, 810−815.

(9) Yu, W.; Liu, M.; Ma, X.; Liu, Z. J. *Colloid Interface Sci.* **1998**, *208*, 439−444.

(10) Pan, C.; Pelzer, K.; Philippot, K.; Chaudret, B.; Dassenoy, F.; Lecante, P.; Casanove, M.-J. *J. Am. Chem. Soc.* **2001**, *123*, 7584−7593.

(11) Pelzer, K.; Vidoni, O.; Phillippot, K.; Chaudret, B.; Colliere, V. *Adv. Funct. Mater.* **2003**, *13*, 118−126.

(12) Yin, Y.; Alivisatos, A. P. *Nature* **2005**, *437*, 664−670.

(13) Xia, Y.; Xiong, Y.; Lim, B.; Skrabalak, S. E. *Angew. Chem., Int. Ed.* **2009**, *48*, 60−103.

(14) Watt, J.; Cheong, S.; Toney, M. F.; Ingham, B.; Cookson, J.; Bishop, P. T.; Tilley, R. D. *ACS Nano* **2009**, *4*, 396−402.

(15) Bakr, O.; Wunsch, B. H.; Stellacci, F. *Chem. Mater.* **2006**, *18*, 3297−3301.

(16) (a) Viau, G.; Brayner, R.; Poul, L.; Chakroune, N.; Lacaze, E.; Fievet-Vincent, F.; Fievet, F. *Chem. Mater.* **2003**, *15*, 486−494. (b) Yin, A.-X.; Liu, W.-C.; Ke, J.; Zhu, W.; Gu, J.; Zhang, Y.-W.; Yan, C.-H. *J. Am. Chem. Soc.* **2012**, *134*, 20479−20489. (c) Hou, Y.; Kondoh, H.; Ohta, T. *Chem. Mater.* **2005**, *17*, 3994−3996. (d) Xu, R.; Xie, T.; Zhao, Y.; Li, Y. *Cryst. Growth. Des.* **2007**, *7*, 1904−1911.

(17) Chang, L. Y.; Barnard, A. S.; Cervera Gontard, L.; Dunin-Borkowski, R. E. *Nano Lett.* **2010**, *10*, 3073−3076.

(18) Lang, B.; Joyner, R. W.; Somorjai, G. A. *Surf. Sci.* **1972**, *30*, 440−453.

(19) Hendy, S.; Brown, S. A.; Hyslop, M. *Phys. Rev. B* **2003**, *68*, 241403−1−241403−4.

(20) Lim, T. H.; McCarthy, D.; Hendy, S. C.; Stevens, K. J.; Brown, S. A.; Tilley, R. D. *ACS Nano* **2009**, *3*, 3809−3813.

(21) Zheng, H.; Smith, R. K.; Jun, Y.; Kisielowski, C.; Dahmen, U.; Alivisatos, A. P. *Science* **2009**, *324*, 1309−1312.

(22) Yuk, J. M.; Park, J.; Ercius, P.; Kim, K.; Hellebusch, D. J.; Crommie, M. F.; Lee, J. Y.; Zettle, A.; Alivisatos, A. P. *Science* **2012**, *336*, 61−64.

(23) Pacholski, C.; Kornowski, A.; Weller, H. *Angew. Chem., Int. Ed.* **2002**, *41*, 1188−1191.

(24) Griffith, W. P. *Platinum Metals Rev.* **2009**, *53*, 209−215.

(25) Bond, G. C. *Platinum Metals Rev.* **2000**, *44*, 146−155.

(26) Bavli, P.; Polturak, E.; Adler, J. *Phys. Rev. B* **2011**, *84*, 235442−1−235442−9.

(27) Liu, X.; Luo, J.; Zhu, J. *Nano Lett.* **2006**, *6*, 408−412.

(28) Jones, M. R.; Macfarlane, R. J.; Prigodich, A. E.; Patel, P. C.; Mirkin, C. A. *J. Am. Chem. Soc.* **2011**, *133*, 18865−18869.

(29) Martin, J. E.; Wilcoxon, J. P.; Odinek, J.; Provencio, P. *J. Phys. Chem. B* **2000**, *104*, 9475−9486.

(30) Liao, H.-G.; Cui, L.; Whitelam, S.; Zheng, H. *Science* **2012**, *336*, 1011−1014.

(31) Xiong, Y.; Xia, Y. *Adv. Mater.* **2007**, *19*, 3385−3391.